Check for updates

S-N curve for full-locked coil ropes

Background to the verification in prEN 1993-1-11:2020

Many steel rope systems are subjected to fluctuating tensile loads and therefore can fail due to fatigue. There are indications that the fatigue resistance of full-locked coil ropes is somewhat lower than that of other types of rope. Fatigue test data on full-locked coil ropes have been collected, but they terminate at different conditions. A semi-empirical model is employed to extrapolate the test results to full failure of the rope. The resulting S-N curve is being adopted for the revision of European standard prEN 1993-1-11.

Keywords full-locked coil rope; fatigue tests; cable; strand; Eurocode 3

1 Introduction

Steel ropes are often used for spanning large distances in engineering structures such as bridges, long-span roofs and lifts. Various types of rope are available, see Fig. 1. The European standard EN 1993-1-11 [1] provides verification rules for the structural design of ropes. One of the verifications concerns the fatigue life, for which an S-N curve is provided.

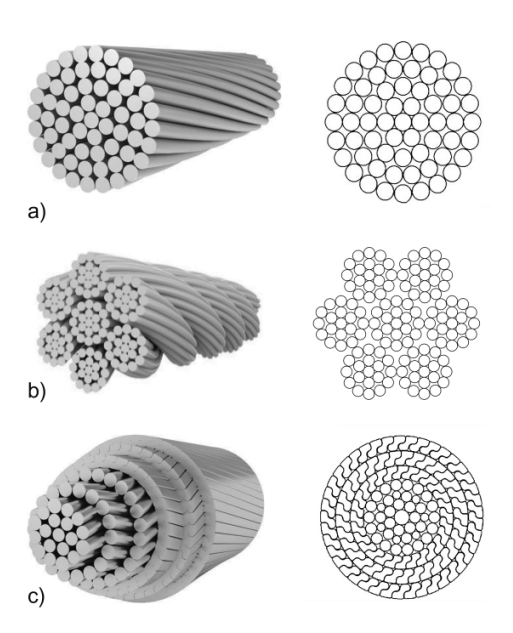


Fig. 1 Rope assemblies (3D figures published by courtesy of Fatzer AG):
a) spiral strand rope, b) stranded rope, and c) full-locked coil rope

This is an open access article under the terms of the Creative Commons Attribution NonCommercial License, which permits use, distribution and reproduction in any medium, provided the original work is properly cited and is not used for commercial purposes

Owing to the lack of background to the S-N curve in the current version of EN 1993-1-11 [1], a study has been carried out to derive such a curve from fatigue tests. There are indications that the fatigue resistance of full-locked coil ropes is lower than that of other types of rope. Therefore, test data on full-locked coil ropes have been collected, see section 2. The tests terminated at different conditions, such as after 2 million applied cycles or (close to) full failure of the rope. They were also carried out at different mean stress levels. A semi-empirical model is developed to account for these differences, see section 3. This resulted in an S-N curve, see section 5, which is proposed for the revised version of EN 1993-1-11, [2]. The current paper provides background to the fatigue resistance of ropes in [2]. It is closely linked to an accompanying paper [3] describing the termination criterion that fulfils the reliability requirements.

2 Fatigue test data on full-locked coil ropes

Most fatigue evaluations of rope systems are based on tests on spiral strand ropes and stranded ropes [3]. The construction of full-locked coil ropes is different from that of spiral strand ropes and stranded ropes, and this may affect the fatigue resistance. The fatigue resistance of individual Z-shaped wires is lower than that of round wires [4]. In a rope, these wires are twisted, and that may further reduce their fatigue resistance. But the contact pressure at the trellis points and the difference in stress between individual wires may be different from those in spiral strand ropes and stranded ropes. This implies that the fatigue resistance and the quantitative effect of the relevant variables distinguished for spiral strand ropes and stranded ropes may be different for full-locked coil ropes. Fevrer [5] provides unpublished data on fulllocked coil ropes of 28 mm diameter which have an endurance that is 55% of that of comparable spiral ropes. However, metal sockets were used for the former, whereas resin sockets were used for the latter, and ropes in resin sockets have a greater endurance. Data on spiral strand ropes in [6] and full-locked coil ropes in [7] are compared in [8], revealing a better fatigue resistance for the former, but the tests employed different termination criterion. A poorer fatigue resistance for full-locked coil ropes is also suggested in [9], but that study was based on a very limited amount of data for full-locked coil ropes. To summarize, the comparisons suggest that locked coil ropes have an inferior fatigue resistance, but the comparisons are subject to debate. This section gives

1

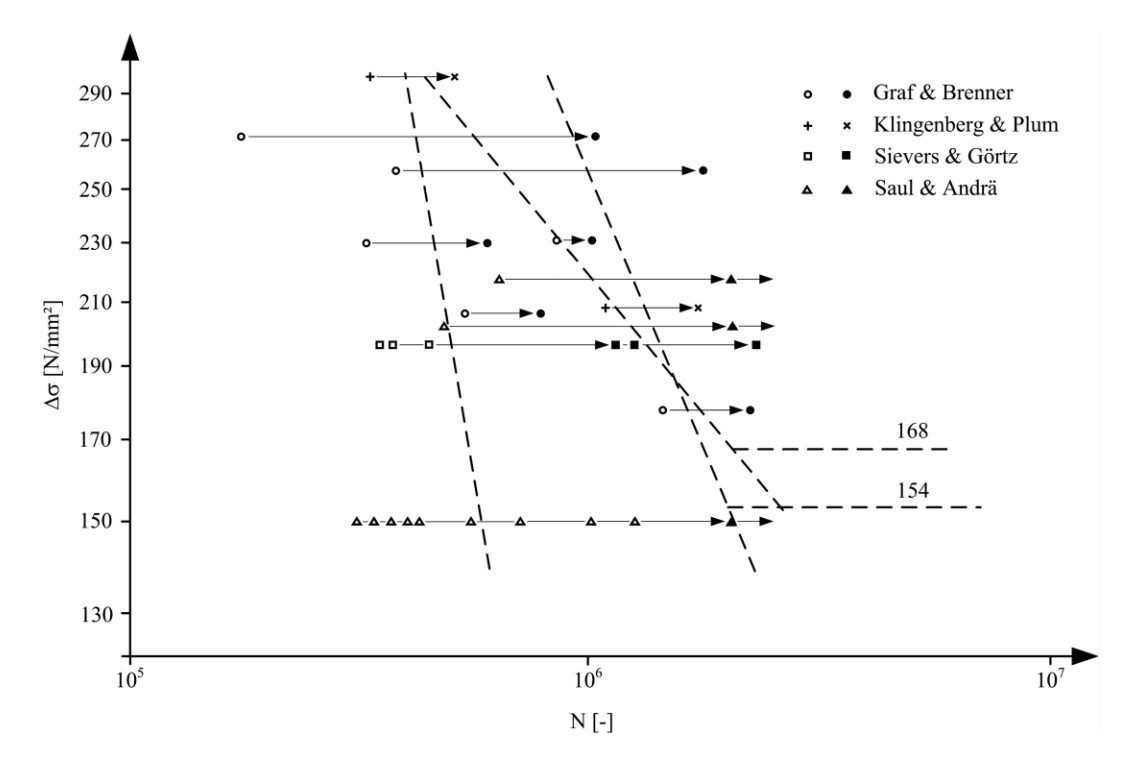


Fig. 2 Test data for full-locked coil ropes collected by Petersen [7] (open symbol = detection of first wire fracture, solid symbol = termination of test)

an overview of the test data collected for full-locked coil ropes.

An increase in rope diameter appears to result in a decrease in the fatigue resistance [3]. Therefore, the fatigue data collected here cover large diameter ropes only. Not much test data on full-locked coil ropes can be found in the literature. All data are evaluated with a simple Basquin relation:

$$\log_{10}\left(N\right) = C_1 - m_1 \log_{10}\left(\Delta\sigma\right) \tag{1}$$

where $\Delta\sigma$ is the stress range (defined as the applied load range divided by the metal area), N is the number of cycles, and C_1 and m_1 are fitting parameters. Petersen [7] presented a collection of data from other German sources, see Fig. 2. Details about the geometry (diameter, lay angle) were not provided. Tracing the original data revealed that most tests were terminated before full failure of the rope. This is not only true for the tests terminated after $2 \cdot 10^6$ cycles, but also for most of the other tests.

Saul and Andrä [10] provided the fatigue resistance of full-locked coil ropes based on the results of various tests. They developed an empirical model and used it to determine the fatigue resistance related to the first wire fracture. They further showed that a relatively large number of wire fractures occur near or even in the socket. This was also observed by Schmidmeier [11] for full-locked coil ropes loaded in bending. Sedlacek et al. [12] and Paschen [13] collected test data from suitability tests on full-locked coil ropes from various sources and refined the model of Saul and Andrä [10]. These suitability tests consist of a fatigue test with $N_{\rm t}=2\cdot 10^6$ cycles with a stress range $\Delta\sigma_{\rm t}=150$ N/mm² and a maximum stress $\sigma_{\rm max}$

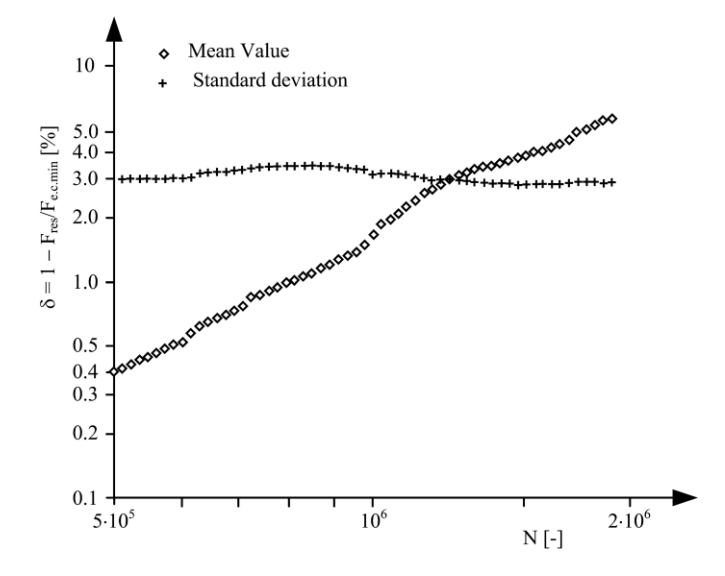


Fig. 3 Mean value and standard deviation for the relation between number of cycles (for a test stress range of 150 N/mm²) and the relative loss of resistance according to Paschen [13]

equal to 42% of the tensile strength of the wire $f_{\rm uk}$. The fatigue test was succeeded by a tensile test to determine the remaining rope resistance $F_{\rm c,min}$.

Based on 15 tests with wire fractures recorded as a function of the number of cycles and a model determining the relative loss of resistance as a function of the number of fractured wires, Sedlacek et al. [12] and Paschen [13] derived a relationship between the relative loss of resistance and the number of cycles, see Fig. 3. Using this graph in combination with a Student's t-distribution, they provided the 95% fraction of the relative loss in rope resistance as a function of the stress range at a life of $2 \cdot 10^6$ cycles.

The analyses of Sedlacek et al. [12] and Paschen [13] are valid for the maximum stress range applied in the suitability tests. There are indications in the literature that the mean stress is highly relevant for fatigue of ropes. Based on a Smith diagram, the following equation for determining the fatigue resistance for a defined stress range of full-locked coil ropes is given in [7]:

$$\Delta \sigma_{\rm R} = \frac{1 - R}{1 - xR} \Delta \sigma_0 \tag{2}$$

with
$$R = \frac{\sigma_{\min}}{\sigma_{\max}} = \frac{\sigma_{\max} - \Delta\sigma}{\sigma_{\max}}$$
 (3)

where:

R load ratio

 $\Delta \sigma_{R}$ fatigue resistance expressed as stress range at stress ratio R

 $\Delta \sigma_0$ equivalent fatigue resistance at R = 0

x parameter to control the influence of load ratio

and wire strength, see [7].

 Tab. 1
 Fatigue test data for large diameter full-locked coil ropes

<i>D</i> [mm]	A _m [mm ²]	<i>f</i> _u [N/mm ²]	$\Delta \sigma_{\rm p}$ [N/mm ²]	R _p	N_1	$N_{ m p}$	P_{fl}	P_{0}	P _t	δ_{p}'	Source
72	3640	1500	70	0.86		1.29E+06	0	0	0	a)	
72	3640	1500	110	0.80	3.19E+05	1.56E+06	3	3	13	10 ^{a)}	[10]
72	3640	1500	70	0.86		1.00E+06	0	0	0	a)	
72	3640	1500	110	0.80	2.58E+05	1.02E+06	0	0	13	10 a)	[10]
80	4350	1600	120	0.78	1.10E+06	2.10E+06	0	0	20	b)	[10]
92	5750	1500	139	0.64	5.68E+05	2.09E+06	1	1	1	1	[10]
54	1975	1500	150	0.74	1.65E+06	2.00E+06	8	5	9	12	[10]
72	3607	1500	152	0.70	4.38E+05	2.21E+06	6		38	22	[10]
72	3607	1500	152	0.70	6.10E+05	2.09E+06	7		35	20	[10]
72	3607	1500	152	0.70	1.07E+06	2.04E+06	1		5	3	[10]
65	2953	1300	179	0.68	1.45E+06	2.10E+06	0	0	27	26	[15]
69	3147	1500	196	0.64	5.44E+05	2.00E+06	73	3	80	16	[10]
104	7504	1530	203	0.06	4.94E+05	2.00E+06			13	5	[10]
65	2953	1300	207	0.65	5.20E+05	7.53E+05	0	0	51	49	[15]
54	1975	1500	209	0.67	1.10E+06	1.61E+06	36		139	100	[16]
73	3738	1300	219	0.51	6.25E+05	2.00E+06	24	0	46	22	[10]
65	2953	1300	230	0.62	3.10E+05	5.88E+05	1		21	20	[15]
65	2953	1300	231	0.03	8.08E+05	9.80E+05	2		205	100	[15]
65	2953	1300	258	0.07	3.65E+05	1.63E+06	55		113	75	[15]
65	2953	1300	272	0.04	1.60E+05	9.71E+05	20		112	75	[15]
54	1975	1500	299	0.59	3.35E+05	4.98E+05	2		61	53	[16]
69			196	0.64	3.87E+05	1.09E+06				b)	[17]
69			196	0.64	3.70E+05	1.19E+06				b)	[17]
69			196	0.64	4.28E+05	2.19E+06				b)	[17]
101	6900	1460	90	0.64	3.00E+07	3.00E+07	0		0	a)	
101	6900	1460	180	0.65	4.00E+06	4.00E+06	0		0	a)	
101	6900	1460	200	0.63	5.75E+05	1.27E+06	5		28	12 a)	[18]
105	7490	1500	150	0.76	3.36E+05	2.00E+06	5	3	30	15	[10]
105	7490	1500	150	0.76		2.00E+06	4	2	4	2	[10]
115	9040	1500	150	0.76	3.60E+05	2.00E+06	15	1	122	52	[10]
115	9040	1500	150	0.76	3.10E+05	2.00E+06	32	0	57	24	[10]
118	9520	1500	150	0.76	3.99E+05	2.00E+06	20	2	65	20	[10]
118	9520	1500	150	0.76	3.96E+05	2.00E+06	21	1	30	9	[10]
118	9520	1500	150	0.76	5.40E+05	2.00E+06	23	0	28	8	[10]
120	9840	1600	150	0.78	1.00E+06	2.00E+06	15	2	16	5	[10]
105	7490	1600	150	0.78		2.00E+06	11	0	86	33	[10]
105	7490	1600	150	0.78	7.04E+05	2.00E+06	32	6	47	18	[10]
118	9520	1570	147	0.77	3.00E+05	2.00E+06			7	2	[13]
118	9520	1570	147	0.77		2.00E+06			0	0	[13]
104	7350	1570	147	0.77	1.10E+06	2.00E+06			1	0	[13]
104	7350	1570	147	0.77	9.70E+05	2.00E+06			12	5	[13]
104	7350	1570	147	0.77	6.10E+05	2.00E+06			13	5	[13]

a) Test carried out at different stress range levels (see rows above and/or below) after no wire fractures in low stress range.

b) Insufficient information available for proper analysis. Data not used in the following statistical evaluation.

This equation can also be found in the old standard, DIN 1073 [14]. The value of x in that standard was derived from two distinct points on the Smith diagram, namely, $\Delta\sigma_0=200$ N/mm², and the suitability test load condition, with $\Delta\sigma_t=150$ N/mm² and a stress ratio $R_t=0.76$ for $\sigma_{\rm max}=0.42f_{\rm uk}$. Assuming a tensile strength $f_{\rm uk}=1500$ N/mm² (a reasonable value for full-locked coil ropes), then $x=(\sigma_{\rm max}-\Delta\sigma_0)/(\sigma_{\rm max}-\Delta\sigma_{\rm R})$, resulting in the value x=0.896.

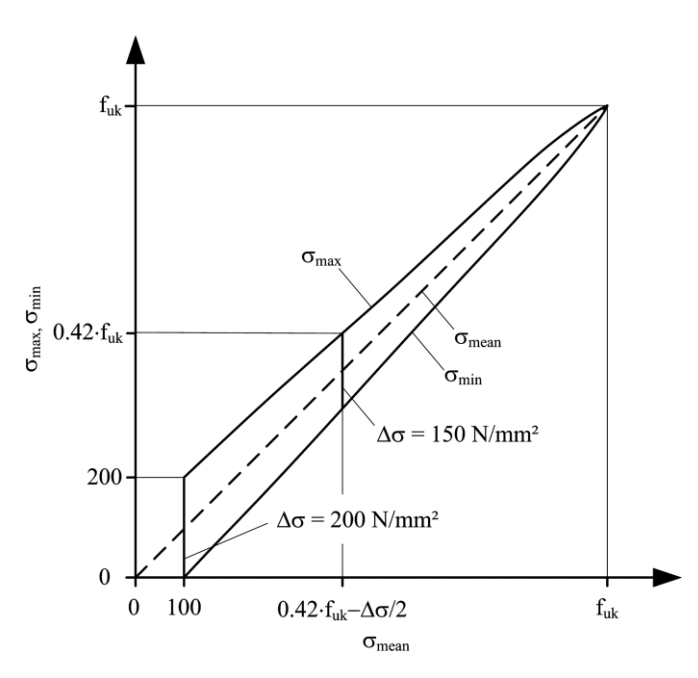


Fig. 4 Smith diagram according to [7]

Tab. 1 and Fig. 5 give an overview of all fatigue test data found for large diameter full-locked coil ropes, where:

A_{m}	metal cross-sectional area
$\Delta\sigma_{ m p}$	stress range
$R_{\rm p}$	stress ratio
$\hat{N_1}$	number of cycles to first wire fracture
$N_{ m p}$	number of cycles to termination of test
$P_{\rm fl}, P_{\rm fo}, P_{\rm t}$	number of fractured wires in free length, in
	outer layer of free length and total fractured wires respectively (all at termination of the
	test)

(δ'_p will be introduced later.)

Most of the test data are from suitability tests, but were not necessarily performed with the stress range and stress ratio according to EN 1993-1-11 [1] or prEN 1993-1-11 [2].

The test data in Fig. 5 show a large scatter, and the scatter is still significant if all data are normalized to a stress ratio R = 0.76 using Eq. (2), see Fig. 6. This is expected to be related to the following:

- From a statistical point of view, the number of cycles to first wire fracture is likely to be related to the total number of wires in the strand, whereas different numbers of wires are used in the data of the figures.
- First wire fracture may be difficult to detect, especially
 if it is a wire in one of the inner layers. The first wire
 fracture data may therefore be unreliable.
- The tests were terminated after different criteria, namely, a cross-section loss between 1% and 100% of the full cross-section. The accompanying paper [3] shows the significance of this parameter.

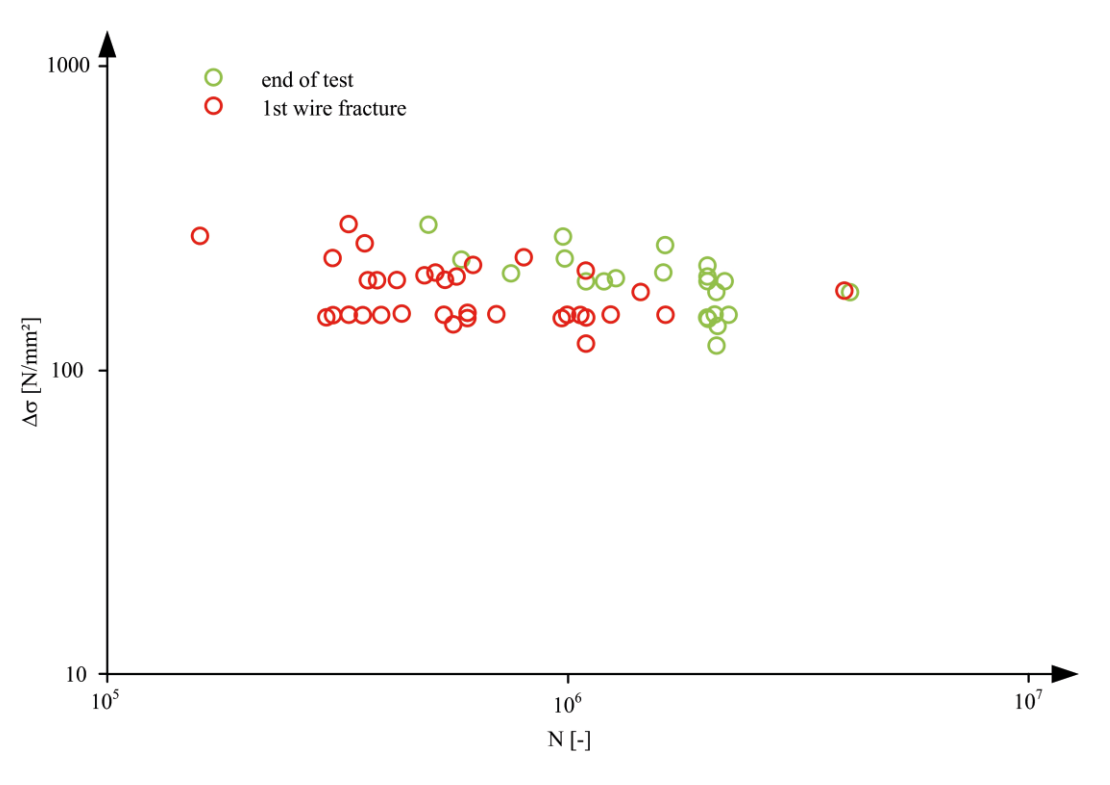


Fig. 5 Fatigue test results collected for full-locked coil ropes

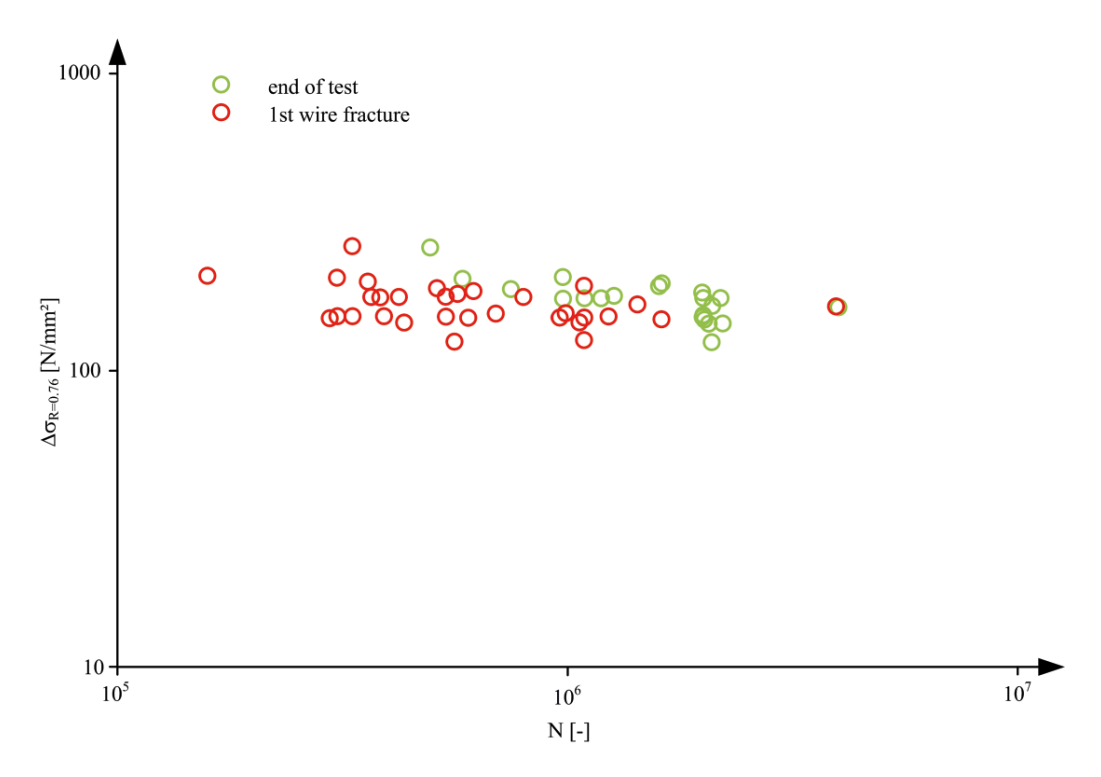


Fig. 6 Fatigue test results collected for full-locked coil ropes, with the stress range normalized to a stress ratio R = 0.76

3 Regression model for fatigue resistance of fulllocked coil ropes

For a proper derivation of the fatigue resistance, it is necessary to use one termination criterion for all tests. The evaluation of the fatigue resistance in the following is based on fatigue failure of the full rope. The accompanying paper [3] demonstrates that an S-N curve derived for full rope failure satisfies the reliability required by EN 1990 [19]. In order to use the test data in conjunction with the termination criterion for failure of the full rope, a model is applied here to extrapolate the test data. The model is a compromise between the challenges of: i) using as much fatigue test data as possible in the statistical evaluation, even if the tests were carried out or terminated according to different criteria, and ii) finding a balance between the accuracy of the model and the number of calibration parameters. The basis is the empirical model of Sedlacek et al. [12] and Paschen [13], with its predecessor by Saul and Andrä [10]. Their model is rewritten in the following form:

$$\delta = a(N_{t})^{b} \tag{4}$$

where δ is the relative loss of residual strength of the rope after the fatigue test (ranging between 0 for an intact strand and 1 for a fully broken strand), $N_{\rm t}$ is the number of cycles in a suitability test according to [1], [2] (with stress range $\Delta\sigma_{\rm t}=150~{\rm N/mm^2})$ and a,b are calibration coefficients to fit the data in Fig. 3, see Tab. 2 (first three columns).

A tensile test was not performed on all specimens after the fatigue test and so δ is not known for all tests. For this reason, the evaluation applied here is related to a parameter δ' , defined as the relative loss of area, i.e. the ratio between the area of broken wires and $A_{\rm m}$. Here, δ' is estimated to be the number of reported fractured wires at $N_{\rm p}$ over the total number of wires in the rope. This assumes that all wires have the same cross-sectional area – which is a reasonable approximation for most of the ropes tested for which such information was available – and that all wires fracture in one recovery length. Even though the test samples are often somewhat longer than one recovery length, the latter assumption is expected to be appropriate because: i) the fractures are often clustered near one of the sockets and ii) tests by Esslinger [20] demonstrate that the fatigue resistance does not vary to a great extent between one and a few recovery lengths. A sensitivity study of this conservative assumption is given at the end of this section.

Knowing that the fatigue resistance depends on the stress ratio, the S-N curve should refer to a specific stress ratio, e.g. R=0 or (as used here) $R=R_{\rm t}=0.76$. Using the Basquin relation (Eq. (1)) and the stress ratio correction (Eq. (2)), it is possible to generalize Eq. (4) for any combination of stress range $\Delta\sigma_R$ and stress ratio R:

$$\delta' = a \left(N \left[\frac{\Delta \sigma_{t}}{\Delta \sigma_{R}} \frac{1 - R}{1 - xR} \frac{1 - xR_{t}}{1 - R_{t}} \right]^{-m_{t}} \right)^{b}$$
 (5)

Tab. 2 Calibration coefficients a,b,a',b', the latter assuming $m_1 = 4$

Definition	$\log_{10}(a)$	b	$\log_{10}(a')$	b ′
Average	-14.56	2.13	-13.83	2.
95% fraction, 75% confidence	-13.46	2.09	-13.02	2.

The derivative of Eq. (5) with respect to the number of cycles (i.e. the rate of relative loss of area) is

$$\frac{d\delta'}{dN} = ab \cdot N^{(b-1)} \left[\frac{\Delta \sigma_t}{\Delta \sigma_R} \frac{1 - R}{1 - xR} \frac{1 - xR_t}{1 - R_t} \right]^{-m_t b}$$
 (6)

Eq. (6) is derived for a relatively small loss of area $(\delta' \le 0.073)$, see Fig. 3). On the other hand, with a relatively large loss of area, an increasing rate $\frac{d\delta'}{dN}$ is expected because the maximum stress and the stress range in the intact wires increase as the number of wire fractures increases. The result of this increasing stress (range) is an increase in the rate of wire fractures towards full fracture, which is also demonstrated in a fatigue test on a full-locked coil rope in [18], see Fig. 7. Further, from a theoretical perspective, the rate should approach asymptotic

behaviour if almost all wires are broken, i.e. $\lim \left(\frac{d\delta'}{dN}\right) = \infty$

if $\delta' \to 1$, because of the increased stress in the remaining wires. In order to use the model for full rope failure tests, the model of [12], [13] therefore needs to be modified.

The model of [12], [13] was modified by incrementally adapting the internal stress range in the intact wires to consider the actual stress instead of the nominal stress, where the actual stress range is equal to $\Delta\sigma/(1-\delta)$, i.e. the stress range increases due to the reduced remaining area of the strand. Eq. (6) is therefore replaced by

$$\frac{d\delta'}{dN} = a'b' \cdot N^{(b'-1)} \left[\frac{\Delta\sigma_{t}}{\Delta\sigma_{R}} \frac{1-R}{1-xR} \frac{1-xR_{t}}{1-R_{t}} \right]^{-m_{t}b'}$$

$$\left[\left(1 - \delta' \right) \right]^{-m_{t}b'}$$
(7)

where coefficients a',b' are slightly different from a,b because an (almost unnoticeable) influence of the loss of wires is already present in the stress range in the remaining wires at the end of the curve in Fig. 3, where $\delta = 0.073$. Coefficients a',b' are a function of the slope parameter m_1 . For this reason, the coefficients have been recalibrated in order to match the relationship of Fig. 3. The fourth and fifth columns of Tab. 2 provide the calibrated values for an assumed slope parameter $m_1 = 4$. Note that Eq. (7) is an estimate, like Eq. (6), where the estimate of Eq. (6) is expected to be too optimistic for fatigue up to full failure.

Integrating Eq. (7) gives

$$\int_{\delta_0'}^{\delta_f'} \left(1 - \delta'\right)^{m_1 b'} d\delta =$$

$$a'b' \left[\frac{\Delta \sigma_t}{\Delta \sigma_R} \frac{1 - R}{1 - xR} \frac{1 - xR_t}{1 - R_t} \right]^{-m_1 b'} \cdot \int_0^{N_f} N^{b'-1} dN$$
(8)

where δ'_0 is the relative loss of area at the start of the fatigue test, δ'_f the relative loss of area at the end of the fatigue life and N_f the number of cycles to failure. Solving Eq. (8) gives

$$N_{\rm f} = \left[\frac{\left(1 - \delta'_{0}\right)^{\left(m_{\rm i}b' + 1\right)} - \left(1 - \delta'_{\rm f}\right)^{\left(m_{\rm i}b' + 1\right)}}{a'\left(m_{\rm i}b' + 1\right) \cdot \left(\frac{\Delta\sigma_{\rm t}}{\Delta\sigma_{\rm R}} \frac{1 - R}{1 - \kappa R} \frac{1 - \kappa R_{\rm t}}{1 - R_{\rm t}}\right)^{-m_{\rm i}b'}} \right]^{1/b'}$$
(9)

Failure is induced, and hence the number of cycles to failure is obtained once the maximum stress level in the remaining wires exceeds the tensile strength of the wires:

$$1 - \delta'_{f} = \frac{\sigma_{\text{max}}}{f_{\text{uk}}} = \frac{\Delta \sigma_{R}}{f_{\text{uk}} (1 - R)}$$
 (10)

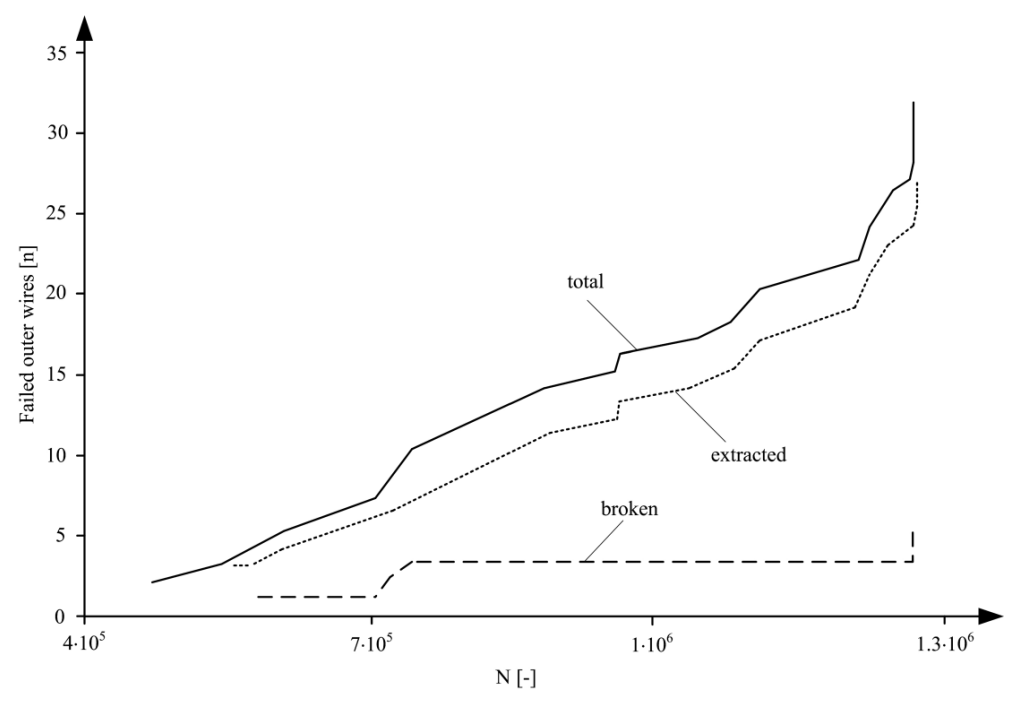
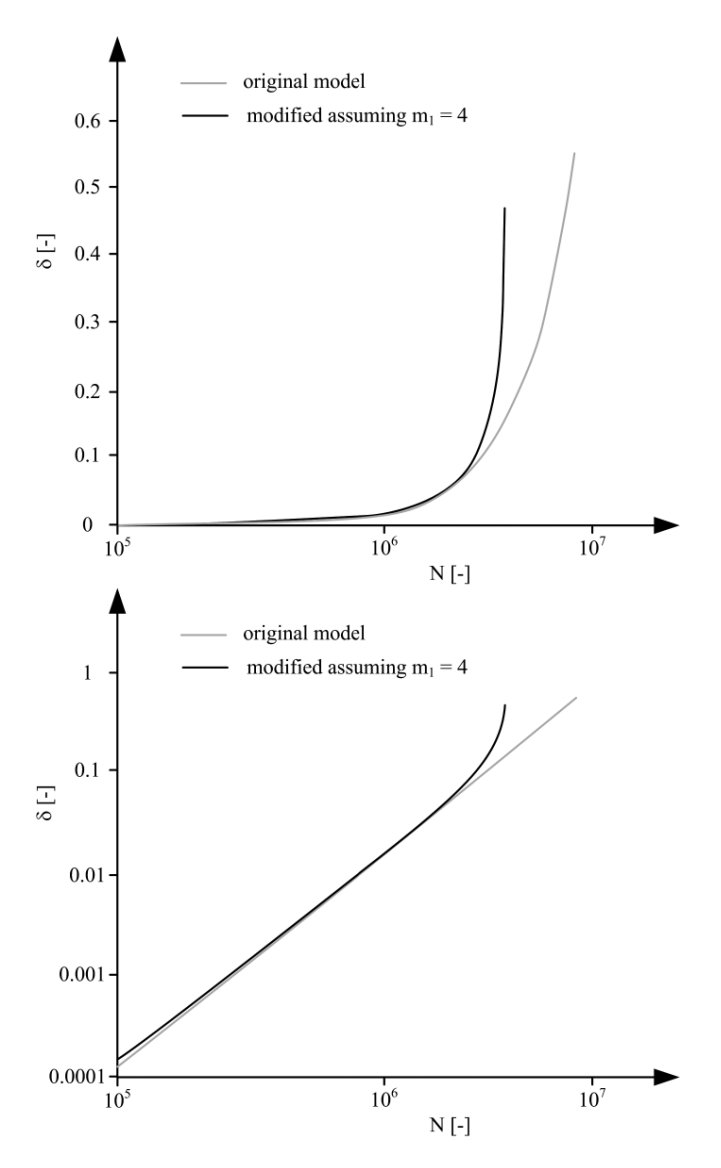


Fig. 7 Number of failed outer (Z) wires as a function of the number of cycles in a test in [18]



 $\begin{array}{ll} \textbf{Fig. 8} & \text{Simulated relative loss of area as a function of number of cycles as} \\ & \text{in a suitability test, i.e. } \Delta\sigma_t = 150 \text{ N/mm}^2 \text{ and } R_t = 0.76 \\ \end{array}$

Substituting Eq. (10) into Eq. (9) allows the number of cycles to failure $N_{\rm f}$ to be determined for any combination of $\Delta\sigma_{\rm R}$ and R. Fig. 8 shows the average relationship between the original model of [12], [13] (Eq. (6)) and the modified version (Eq. (7)), assuming $m_1=4$, with test conditions as in a suitability test. The figure shows the same trend in relative loss of area compared with the test in Fig. 7.

The model is used to estimate the number of cycles to failure of the full-locked coil rope fatigue tests. This is done in two steps:

1 The initial condition is an undamaged strand, i.e. $\delta_0 = 0$. Using Eq. (9), the estimator \tilde{a} of variable a' is determined based on the test database by using

$$\tilde{a} = \frac{1 - \left(1 - \delta'_{p}\right)^{\left(m_{1}b' + 1\right)}}{N_{p}^{b'}\left(m_{1}b' + 1\right) \cdot \left(\frac{\Delta\sigma_{t}}{\Delta\sigma_{p}} \frac{1 - R_{p}}{1 - xR_{p}} \frac{1 - xR_{t}}{1 - R_{t}}\right)^{-m_{1}b'}}$$
(11)

where $\Delta \sigma_{\rm p}$ and $R_{\rm p}$ are the control parameters of that specific test according to Tab. 1, $N_{\rm p}$ is the total number of cycles in the specific test and $\delta'_{\rm p}$ is the relative loss of area at the end of the specific test.

2 The test data are extrapolated to the full failure condition using the equivalent of Eq. (10):

$$N_{\rm p} + \left[\frac{\left(1 - \delta_{\rm p}\right)^{\left(m_{\rm l}b' + 1\right)} - \left(\frac{\Delta\sigma_{\rm p}}{f_{\rm uk}\left(1 - R_{\rm t}\right)}\right)^{\left(m_{\rm l}b' + 1\right)}}{\tilde{a}\left(m_{\rm l}b' + 1\right) \cdot \left(\frac{\Delta\sigma_{\rm t}}{\Delta\sigma_{\rm p}} \frac{1 - R_{\rm p}}{1 - \kappa R_{\rm p}} \frac{1 - \kappa R_{\rm t}}{1 - R_{\rm t}}\right)^{-m_{\rm l}b'}} \right]^{1/b'}$$
(12)

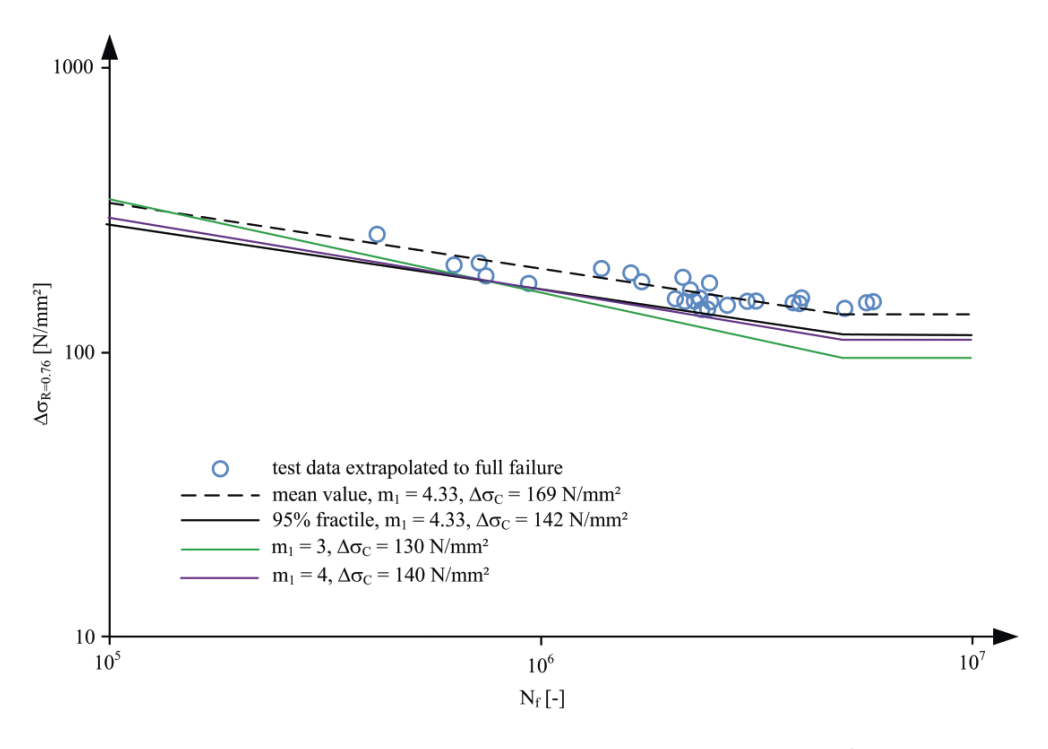


Fig. 9 Evaluation of the fatigue test data for full-locked coil ropes extrapolated to full fracture (DC = detail category, referring to full rope fracture)

Fig. 9 shows the results of all test data extrapolated to full failure, using the standard value for the stress ratio $R_{\rm t}=0.76$ and excluding: i) tests with zero wire fractures (i.e. excluding run-outs), ii) tests that were re-run (re-inserted) at a higher stress range after a first fatigue test without fractured wires, and iii) one test with the indication 'Probe krumm' ('sample crooked') [13]. In total, 29 tests then remain.

A large reduction in the scatter compared with the original data (Fig. 5) is visible in Fig. 9. The remaining standard deviation of the 10th base logarithm of N is s = 0.19. This is a realistic value for the aleatory scatter in fatigue data and comparable with the scatter of individual test series on a single rope system in [21]. The number of remaining datasets, 29, is sufficient for deriving a characteristic S-N curve. The same procedure as used to obtain the characteristic S-N curves of the details in EN 1993-1-9 [22] is applied here to obtain the characteristic S-N curve, defined as the one-sided lower 95% prediction bound [23]. Fig. 9 gives the resulting characteristic S-N curves for a free slope and for predefined, fixed slopes $m_1 = 3$ and $m_1 = 4$. The $\Delta \sigma_{\rm C}$ values in the legend refer to the characteristic fatigue resistance in N/mm² at 2·10⁶ cycles. The resulting free slope $m_1 = 4.33$ is close to – and for practical conditions slightly more beneficial than – the slope $m_1 = 4$ as adopted in EN 1993-1-11 [1], whereas the corresponding value $\Delta \sigma_{\rm C}$ = 142 N/mm² is slightly lower when compared with the value $\Delta \sigma_{\rm C} = 150 \text{ N/mm}^2 \text{ in EN } 1993\text{-}1\text{-}11$ [1]. Fig. 9 was generated for the mean stress influence factor x = 0.896 mentioned previously. Optimizing the fit with this factor with both m_1 and x as unknowns gives a best fit factor x = 0.917, $m_1 = 4.06$ and $\Delta \sigma_C = 142 \text{ N/mm}^2$. Hence, the factor x in [14] fits the data well.

As a validation of the model, the extrapolation to $N_{\rm f}$ using Eq. (12) for test data with $\delta_p' < 0.5$ is compared with the specimens that were tested to (almost) full failure, i.e. the data with $\delta'_p \ge 0.5$. Fig. 10 illustrates the comparison. Note that the squares in the figure indicate the actual number of tested cycles of the data with $\delta_p' \ge 0.5$, i.e. no extrapolation with Eq. (12). The data fall in the same scatter band, indicating that the extrapolation using Eq. (12) is appropriate. As a reference, the data of Casey [6] covering large diameter spiral strands and stranded ropes were also added to the figure (not corrected for stress ratio), thus demonstrating that full-locked coil ropes do indeed have the lowest fatigue resistance of the three types of rope. The model is also applied to extrapolate the test data to a criterion of 5% fractured wires and compared with tests that were terminated at that condition, see Fig. 11. Again, good agreement was obtained. For this condition, $\Delta \sigma_{\rm C} = 116 \, \rm N/mm^2$, i.e. 20% lower than full fracture, m_1 = 4.33 and s = 0.21.

Finally, the sensitivity to the assumption at the start of this section is considered, namely, that all fractured wires are considered in δ' irrespective of the location of the fracture. The analysis is redone but now assuming that the fractures are equally distributed between the two socket regions and that the wires fractured near one socket are fully effective at the other socket (i.e. the specimen is longer than one recovery length). The resulting S-N curve has the parameters $m_1 = 4.44$ and $\Delta \sigma_{\rm C} = 149$ N/mm². The effect of the assumption is thus small.

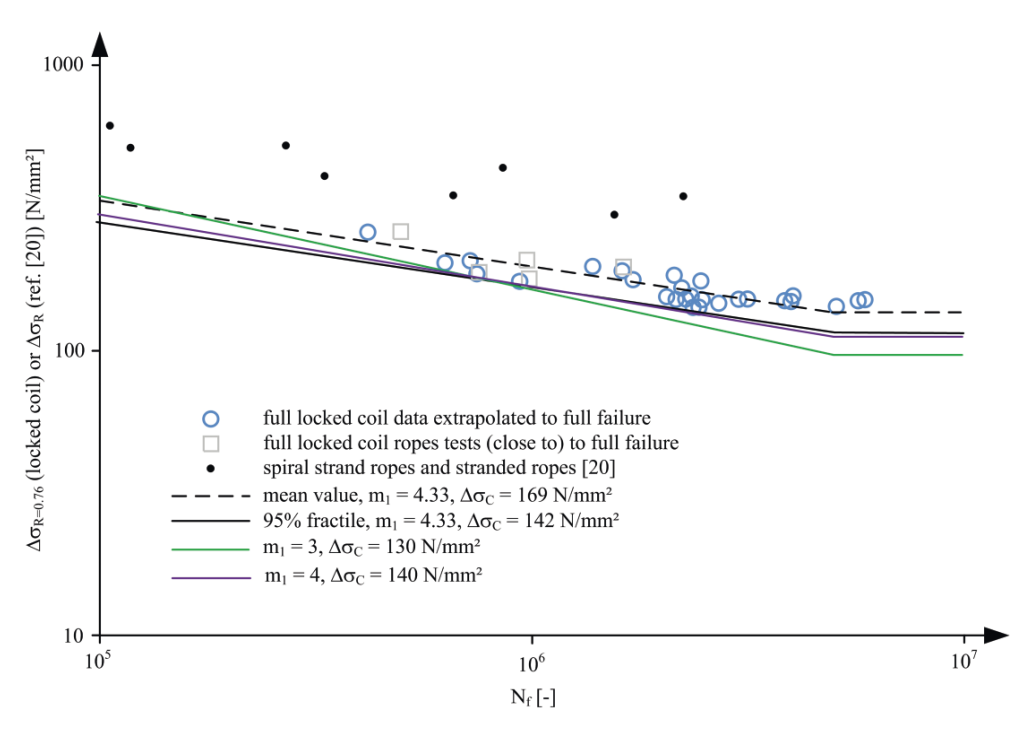


Fig. 10 Fatigue test data extrapolated to full failure compared with the specimens that were tested to (almost) full failure (DC = detail category, referring to full rope failure)

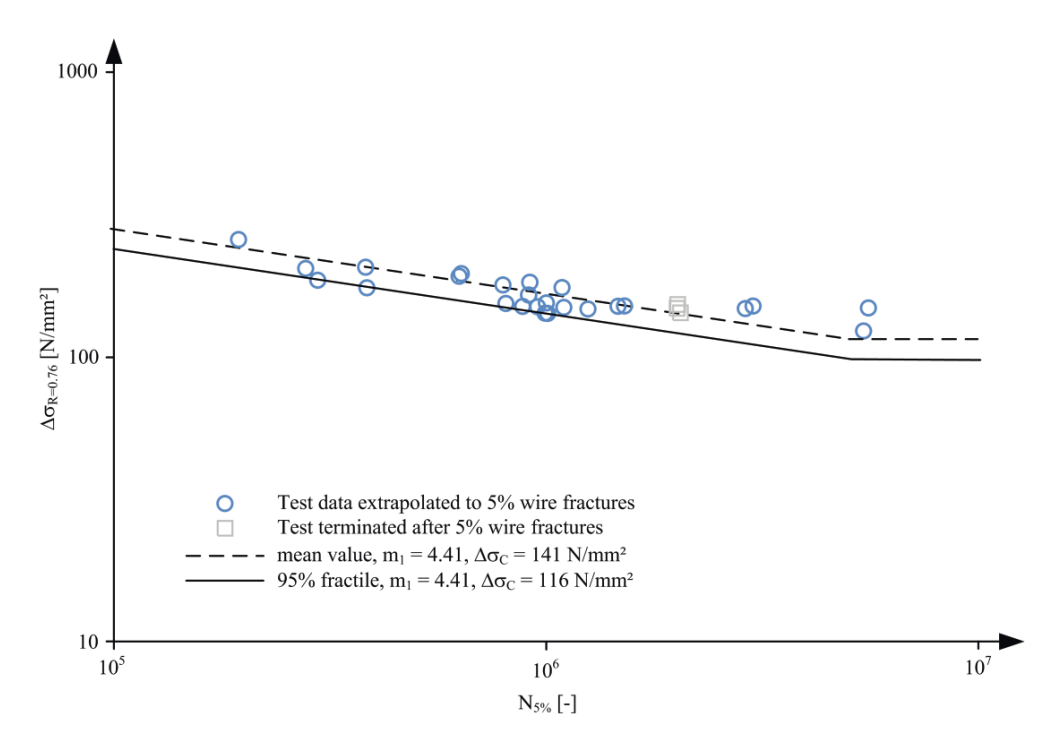


Fig. 11 Evaluation of fatigue tests with 5 % of wires fractured

4 Discussion of the results

The resulting value of the fatigue resistance at $2 \cdot 10^6$ cycles as derived for full rope failure, $\Delta \sigma_C = 142$ (or 149) N/mm², is close to the stress range $\Delta \sigma_t = 150 \text{ N/mm}^2$ used in the suitability test. The suitability criterion in [1], [2] also implies that the rope must have a considerable residual strength $F_{\text{res}} \ge 0.92 F_{\text{c.min}}$, in turn implying that the specimen is not close to failure at the end of the fatigue part of the suitability test. Further, the suitability criterion provided is such that rope systems designed with reasonable care will satisfy it, i.e. the average resistance will be higher than the criterion and it is therefore not unusual for the characteristic fatigue strength to appear to be close to the suitability criterion. Finally, the conditions of the suitability tests are considered to be conservative for almost all practical situations; for a more likely (average) stress ratio R = 0.4 in practice instead of R = 0.76 applied in the suitability tests and used to derive the S-N curve, Eq. (2) results in a 25% higher fatigue resistance. Suitability tests are still considered crucial, because the derived characteristic S-N curve is based on rope systems that have passed the suitability criterion. For convenience, a rounded value $\Delta \sigma_{\rm C} = 145 \text{ N/mm}^2$ is adopted in [2]. The curve appears to be conservative for spiral strand ropes and stranded ropes with a large diameter. The curve is also deemed to be conservative for small diameter ropes.

Owing to a lack of data, conventions must be applied to the number of cycles at the knee-point N^* and the slope parameter of the second part of the S-N curve. This second part is associated with damage introduced by variable-amplitude loading. A limited number of tests have been performed on ropes with variable-amplitude loading, basically consisting of blocks with constant amplitude [6], [24]. The data – all from spiral strand ropes –

show that the cumulative damage rule of Palmgren-Miner [25] gives a reasonable estimate of the life [5]. However, the fraction of the damage created in the second branch of the S-N curve is too small for estimating N^* and m_2 . In prEN 1993-1-9:2020 [26], N^* depends on the type of detail and values of 2 · 106, 5 · 106 and 107 cycles are proposed for non-welded details, welded details with a high fatigue resistance and welded details with a low fatigue resistance respectively. Many suitability tests contain fractured wires in a stress range that is just a little higher than the 2·10⁶ cycles of the proposed S-N curve. Hence, it is likely that $N^* > 2 \cdot 10^6$. A value $N^* = 5 \cdot 10^6$ cycles is proposed here. This value might be (slightly) conservative but this seems appropriate considering the lack of data and the observation that N^* may increase with rope length [3]. It means that the 95% fraction of the stress range at the knee-point is $\Delta \sigma^* = 115$ MPa. Haibach's proposal [27] is often applied for slope parameter m_2 , i.e. $m_2 = 2m_1 - 1$. However, considering the limited amount of proof, it is proposed to use the same slope parameter as in [1] as a conservative figure, namely, $m_2 = m_1 + 2$. For $m_1 = 4$ this gives $m_2 = 6$. Fig. 12 shows the S-N curve finally selected for the updated standard [2], together with the S-N curve in the original standard [1] and a previous alternative according to [8].

The S-N curve is valid for fluctuating tension. In practical applications, the terminations should be carefully designed in order to prevent additional stresses in the socket region, since they may lead to a decrease in the fatigue life, which is not accounted for in the fatigue tests and hence in the S-N curve. One of the most recent and extensive studies into bending fatigue of full-locked coil ropes in bridges is that by Schmidmeier [11]. He concludes that the influence of bending on the fatigue performance is limited in the case of proper anchorage details that allow

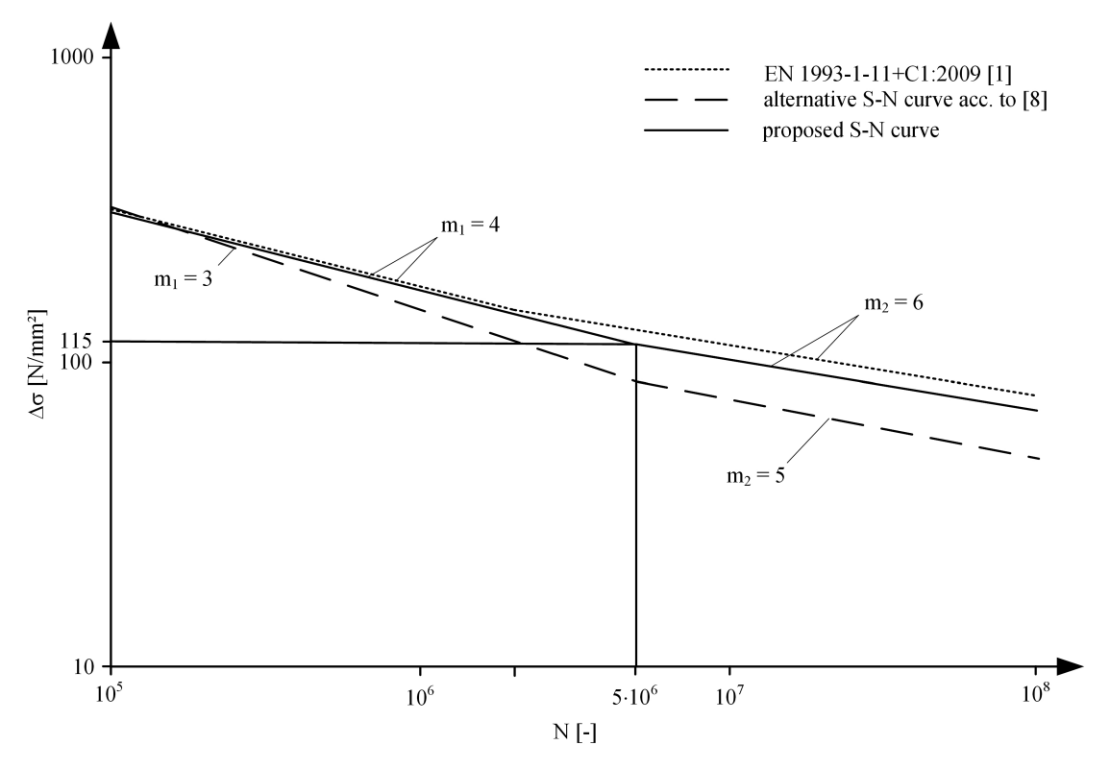


Fig. 12 S-N curves according to [1] and [8], the proposed curve for variable-amplitude loading

for flexibility. Finally, the risk of corrosion or corrosion fatigue of ropes must be considered [13]. This is not accounted for in the proposed S-N curve.

5 Conclusions

A database was collected concerning fatigue test results on large diameter full-locked coil ropes. These tests were carried out at different mean stress levels and (mostly) terminated before full failure. The data were corrected for mean stress – which appears to be significant for this type of rope – and a semi-empirical model was employed to extrapolate the test data to full failure. The evaluation allows the following conclusions to be drawn:

The resulting, realistic value of 19% for the standard deviation of the logarithm of the number of cycles to failure and the good agreement between test results and predictions at 5% and 100% wire factures demonstrate the validity of the semi-empirical extrapolation model.

- The resulting S-N curve has a slope parameter $m_1 = 4$ and a stress range $\Delta \sigma_{\rm C} = 145 \text{ N/mm}^2$ (rounded value) at a 95% fraction of 2·10⁶ cycles for a stress ratio R = 0.76.
- The fatigue resistance in terms of stress range is 20% lower if a termination criterion of 5% fractured wires is adopted.
- The fatigue resistance in terms of stress range is approx. 25% higher if a stress ratio R = 0.4 is adopted.
- The fatigue resistance of full-locked coil ropes (at R = 0.76) appears to be lower than that of spiral strand ropes and stranded ropes.

Acknowledgements

We would like to thank the members and experts of committee CEN TC250/SC3/WG11, responsible for developing prEN 1993-1-11, for the discussions that initiated this research. The Dutch Road Authority, Rijkswaterstaat, is acknowledged for its financial support of this study.

References

- [1] EN 1993-1-11+C1 (2009) Eurocode 3: Design of steel structures Part 1-11: Design of structures with tension components. Brussels: CEN.
- [2] prEN 1993-1-11 (2020) Eurocode 3: Design of steel structures Part 1-11: Design of structures with tension components. 2nd draft for enquiry. Brussels: CEN.
- [3] Maljaars, J.; Misiek, T. (2021) Fatigue resistance of steel ropes: failure criterion Background to the verification in
- prEN 1993-1-11:2020 in: Steel Construction (accepted for publication). https://doi.org/10.1002/stco.202000058.
- [4] Gabriel, K.; Dillmann, U. (1983) Hochfester Stahldraht für Seile und Bündel in der Bautechnik. Düsseldorf: Werner.
- [5] Feyrer, K. (2015) Wire ropes tension, endurance, reliability.2nd ed. Heidelberg: Springer.
- [6] Casey, N. F. (1993) The fatigue endurance of wire ropes for mooring offshore structures in: Proc. of Round Cable Conf.

- on Applications of Wire Rope Endurance Research. Organisation Internationale Pour L'Etude de L'Endurance des Cables (OIPEEC), Round Table Conf., Delft, pp. 24–49.
- [7] Petersen, C. (2013) Stahlbau Grundlagen der Berechnung und baulichen Ausbildung von Stahlbauten. 4th ed. Wiesbaden: Springer.
- [8] Annan, R. et al. (2020) Revision of EN 1993-1-11 fatigue design rules for tension components in: Steel Construction 13, pp. 61–75.
- [9] HSE (authors unknown) (1997) Review of tension-tension fatigue performance of wire ropes. Health & Safety Executive, Offshore Technology Report OTO 97 080.
- [10] Saul, R.; Andrä, W. (1981) Zur Berücksichtigung dynamischer Beanspruchungen bei der Bemessung von verschlossenen Seilen stählerner Straβenbrücken in: Die Bautechnik 4, pp. 116–124.
- [11] Schmidmeier M. (2016) Zur Ermüdungssicherheit vollverschlossener Seile unter Biegun in: Mitteilungen, No. 102. Karlsruhe: Bundesanstalt für Wasserbau (BAW). https://izw. baw.de/publikationen/mitteilungsblaetter/0/BAWMittei lungen_102_INTERNET.pdf
- [12] Sedlacek, G.; Lopetegui, J.; Neuenhaus, D.; Merzenich, G.; Heinemeyer, C.; Kuck, J. (1995) Untersuchungen zum Schwingungs- und Ermüdungsverhalten der Seile und Kabel abgespannter Brücken mit Fußpunkterregung. RWTH Aachen, Final report for DFG research project SE 351/10-2.
- [13] Paschen, M.; Dürrer, F.; Rentmeister, F. E. (2020) Ermüdungssicherheit von vollverschlossenen Seilen mit Korrosionsschäden BASt-Bericht B 146. Bergisch Gladbach: Bundesanstalt für Straßenwesen, https://bast.opus.hbz-nrw.de/frontdoor/index/index/docId/2336.
- [14] DIN 1073 (1974). Stählerne Straßenbrücken Berechnungsgrundlagen Erläuterungen. Berlin: DIN.

Authors

Prof. Dr. ir. Johan Maljaars (corresponding author) j.maljaars@tno.nl TNO PO Box 155 2600 AD Delft, the Netherlands also: Eindhoven University of Technology, The Netherlands Tel. +31 652803581

Dr.-Ing. Thomas Misiek thomas.misiek@breinlinger.de Breinlinger Ingenieure Kanalstraße 14 78532 Tuttlingen, Germany

- [15] Graf, O.; Brenner, E. (1941) Versuche mit Drahtseilen für eine Hängebrücken in: Bautechnik 19, pp. 410–415.
- [16] Klingenberg, W.; Plum, A. (1955) Versuche an den Drähten und Seilen der neuen Rheinbrücke in Rodenkirchen bei Köln in: Stahlbau 24, pp. 265–272.
- [17] Sievers, H.; Görtz, W. (1956) Der Wiederaufbau der Straßenbrücke über den Rhein zwischen Duisburg-Ruhrort und Hornberg in: Stahlbau 25, pp. 77–88.
- [18] Dijkstra, O. D.; Van Dooren, F. D. (1997) Fatigue test of a large diameter steel wire rope of a cable-stayed bridge in: IABSE reports 76, pp. 171–180.
- [19] EN 1990+A1+C2. (2011) Eurocode: Basis of structural design. Brussels: CEN.
- [20] Esslinger, V. (1992) Fatigue testing of wires and strands. IABSE Workshop, Madrid.
- [21] Chaplin, C. R. (1995). Prediction of the fatigue endurance of ropes subject to fluctuating tension in: IOPEEC bulletin 70, pp. 31-40.
- [22] EN 1993-1-9+C2 (2012) Eurocode 3: Design of steel structures Part 1-9: Fatigue. Brussels: CEN.
- [23] Euler, M.; Kuhlman, U. (2013) Statistical intervals for evaluation of test data acc. to Eurocode 3 Part 1-9. Stuttgart University.
- [24] Rossetti, U., Maradei, F. (1992) Check on the validity of the Miner's hypothesis for tension tension fatigue in: OIPEEC Bulletin 64, pp. 23–28.
- [25] Miner, M. A. (1945) Cumulative damage in fatigue in: J. Appl. Mech. Trans. ASNE 67, pp. 159–164.
- [26] prEN 1993-1-9 (2020) Eurocode 3: Design of steel structures – Part 1-9: Fatigue. 2nd draft for enquiry. Brussels: CEN.
- [27] Haibach, E. (1989) *Betriebsfestigkeit*. Düsseldorf: VDI Verlag GmbH.

How to Cite this Paper

Maljaars, J.; Misiek, T. (2021) S-N curve for full-locked coil ropes – Background to the verification in prEN 1993-1-11:2020. Steel Construction. https://doi.org/10.1002/stco.202100009

This paper has been peer reviewed. Submitted: 10. November 2020; accepted: 2. March 2021.